HEFAT2014
10th International Conference on Heat Transfer, Fluid Mechanics and Thermodynamics
14 – 26 July 2014
Orlando, Florida

ANALYTICAL THERMAL AND COST OPTIMIZATION OF MICRO-STRUCTURED PLATE-FIN HEAT SINK

Rezania A.* and Rosendahl L.A.
*Author for correspondence
Department of Energy Technology,
Aalborg University,
Aalborg 9220,
Denmark,
E-mail: alr@et.aau.dk

ABSTRACT

Microchannel heat sinks have been widely used in the field of thermo-fluids due to the rapid growth in technological applications which require high rates of heat transfer in relatively small spaces and volumes. In this work, a micro plate-fin heat sink is optimized parametrically, to minimize the thermal resistance and to maximize the cost performance of the heat sink. The width and the height of the microchannels, and the fin thickness are analytically optimized at a wide range of pumping power. Using an effective numeric test, the generated equations also discuss the optimum parameters at three sizes of the substrate plat of the heat sink. Results show that, at any pumping power there are specific values of the channel width and fin thickness which produce minimum thermal resistance in the heat sink. The results also illustrate that, a larger channel width and a smaller fin thickness lead to a better cost performance, and the optimum channel height decreases when the pumping power increases.

INTRODUCTION

Microchannel heat sinks, which typically contain a large number of parallel micro plate-fins with a hydraulic diameter on the order of 10 to 1,000 μm, have been recently applied in the automotive, chemical, food, environmental technology, aviation, and space industries [1] and thermoelectric power generation systems [2]. A limiting factor in thermal systems with high heat dissipation rate is effective heat exchanger design, and for this reason, microscale single-phase heat transfer is widely used in industrial and scientific applications [3]. In recent years, many studies have been performed in the field of thermo-fluids to optimize the geometrical parameters of the heat sinks at the micro-scale level. The studies indicate that, the geometric configuration of the microchannel heat sink has a critical effect on the convective heat transfer of the laminar flow in the heat sink [4].

NOMENCLATURE

A	$[\mathrm{m}^2]$	area
b	[m]	fin thickness
C_P	$[\mathrm{J/kg^1.K^1}]$	specific heat of water
D_h	[m]	hydraulic diameter of the channel
H	[m]	channel height
h	$[\mathrm{W/m^2.K^1}]$	heat transfer coefficient
k	$[\mathrm{W/m^1.K^1}]$	thermal conductivity
L	[m]	heat sink length
M	[kg]	heat sink mass
$\dot{m}$	$[\mathrm{kg/s^1}]$	mass flow rate
N	[-]	number of channels in heat sink
Nu	[-]	Nusselt number
Δp_{ch}	[Pa]	pressure drop
Pr	[-]	Prandtl number
P	$[\mathrm{W/kg^1.K^1}]$	cost performance
Re	[-]	Reynolds number
R_{th}	$[\mathrm{K/W^1}]$	heat sink thermal resistance
t	[m]	substrate plate thickness
u	$[\mathrm{m/s^1}]$	fluid velocity
U	$[\mathrm{W/K^1}]$	heat sink thermal conductance
W	[m]	heat sink width
w	[W]	pumping power
Greek symbols		
δ	[m]	channel width
η	[-]	efficiency
μ	$[\mathrm{N.s/m^2}]$	dynamic viscosity
ρ	$[\mathrm{kg/m^3}]$	density
Subscripts		
ch		channel
hs		heat sink
f		fluid
fin		fin
o		overall
pl		plenum
s		substrate plate
t		total

th		thermal

In case of power systems the greatest problem nowadays is not only the huge amount of heat dissipation, but mainly the density of the heat dissipation at the surface of the system structure. Therefore, the main challenge is to design an effective heat exchanger within typical microelectronic's packaging sizes [5].

For achieving overall heat transfer enhancement rectangular microchannels are satisfactory and its heat transfer coefficient is the highest amongst trapezoidal and triangular shaped microchannels [6]. Furthermore, Kroeker et al. [7] found that, on the basis of equal hydraulic diameter and equal Reynolds number, a rectangular channel has less thermal resistance compared with heat sinks with circular cross section channel. The rectangular channel requires more pumping power than the circular channel. By investigating the effect of the channel width and height on the thermal resistance of the heat sink, and based on the theory of a fully developed flow, Kou et al. [8] derived an expression for the pressure drop in microchannels for required pumping power. Their results show that a larger flow area and pumping power can obtain lower thermal resistance. Furthermore, for a single microchannel, they found that, the optimum channel width strongly depends on the channel height when the pumping power is lower than 10^{-3} W.

For decreasing the convective resistance at a given substrate area, both of the convective heat transfer coefficient and the surface area of the channel walls in contact to the fluid should increase [9]. One way to increase the convective heat transfer coefficient is to reduce the hydraulic diameter of the microchannels. On the other hand, for a given pump power, when the hydraulic diameter decreases, the heat resistance of the heat sink increases due to rapidly decreasing of the volumetric flow rate. The optimum channel dimensions can be optimized at a practical limit on the available pumping power by minimizing sum of the convective resistance and the heat resistance ([10], [11]). At a constant pumping power, when the aspect ratio of the channel (the ratio of the channel height to the channel width) becomes larger, the heat transfer area increases but the volumetric flow rate and the fin efficiency decrease.

In the power generation systems, a key factor is the optimization of the systems design, together with its heat source and heat sink. Full thermal optimization yields a simple analytical expression for optimum design [12]. Based on this model, the thermal resistance of the micro heat exchanger can be optimized to maximize the cost performance of systems. In addition, the thermal resistance of the microchannel heat sink can be minimized for a set of aspect ratio [13]. In this study, a micro plate-fin heat sink is optimized parametrically, to minimize the thermal resistance and to maximize the cost performance of the heat sink. The width and the height of the microchannels, and the fin thickness are analytically optimized at a wide range of pumping power. In addition, using an effective numeric test, the generated equations also discuss the optimum parameters at three sizes of the substrate plat of the heat sink. Figure 1 shows the schematic of the heat sink, where water is used for the coolant fluid and the fluid path is made of parallel aluminum channels.

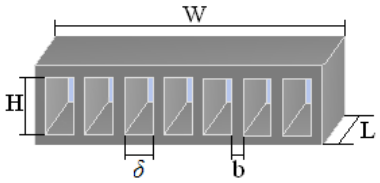

Figure 1 Schematic of the heat sink.

MATHEMATICAL CORRELATIONS

The optimum channel width and the fin thickness together with the heat sink width can define the optimal number of the channels. With the fixed heat sink width, the number of the channels is:

$$N = \frac{W}{b + \delta} \tag{1}$$

where thickness of the heat sink side walls is neglected. The thermal resistance of the heat sink is independent of the level of the dissipated power in forced convection cooling, and is the sum of the conductive resistance (due to conduction through the substrate), heat resistance (due to heating of the coolant fluid as it absorbs energy passing through the heat sink) and convective resistance (due to convection from the heat sink to the coolant fluid) [9]. Temperature range of the working fluid, which is water, indicates that $\Pr > 5$ throughout this study. Prandtl number (Pr) is the ratio of momentum diffusivity to thermal diffusivity. Thus, assuming thermally fully developed flow is acceptable [9]. In addition, for a constant heat flux boundary condition, the temperature difference between the heat sink base and the bulk coolant fluid is the same at any plane in the flow direction [14]. Therefore, the thermal resistance of the heat sink is:

$$R_{th} = \frac{t}{k_{hs} A_s} + \frac{1}{\dot{m} C_p} + \frac{1}{\eta_o h_{fin} A_{fin}} \tag{2}$$

where the first, second and third terms on the right side are conductive resistance, the convective resistance and the heat resistance, respectively. The mass flow rate and the fin area can be defined based on number of microchannels as follows:

$$\dot{m} = \rho_f N \delta H u \tag{3}$$

$$A_{fin} = 2N(H + \delta)L \tag{4}$$

and the convective heat transfer coefficient is:

$$h_{fin} = \frac{Nuk_f}{D_h} \tag{5}$$

Although the Nusselt number is constant in the fully developed laminar flow, it depends on the wall thermal boundary condition and aspect ratio of rectangular channel. For a constant heat flux boundary condition, the variation of the Nusselt number is expressed as follows [15]:

$$\mathrm{Nu} = 8.235 \left(\begin{array}{c} 1 - 2.0421 \left(\frac{\delta}{H}\right) + 3.0853 \left(\frac{\delta}{H}\right)^2 - \\ 2.4765 \left(\frac{\delta}{H}\right)^3 + 1.0578 \left(\frac{\delta}{H}\right)^4 - 0.1861 \left(\frac{\delta}{H}\right)^5 \end{array} \right) \tag{6}$$

In case that the heat sink is located very near to the heat source, the conductive resistance is very small. In this study, the thickness of the substrate plate is 100 μm with a high thermal conductivity (220 W/m.K). With this thickness for the

aluminum substrate, that has a high thermal conductivity, the conductive resistance is %1 of the convective resistance for $t = 200$ μm, and can be neglected.

For the modeling of the convective resistance, the heat conduction in the fins are assumed to be one dimensional only along the fin height, constant heat transfer coefficient, and uniform fluid temperature. The convective resistance can be divided to a correction factor (fin efficiency) to take into account the thermal resistance of the fins, which implies a non-uniform temperature up the walls. The efficiency for straight rectangular low-thickness fin with an adiabatic tip is defined as follows [16]:

$$\eta_{fin} = \frac{tanh\left(\sqrt{2h/k_f b}\, H\right)}{\sqrt{2h/k_f b}\, H} \tag{7}$$

and the overall surface efficiency of the heat sink is:

$$\eta_o = 1 - \left(\frac{NA_{fin}}{A_t}\right)\left(1 - \eta_{fin}\right) \tag{8}$$

Volumetric flow rate in the channels is found straight forward by the product of velocity and cross section area. Therefore, the pumping power to circulate the coolant fluid in the heat sink is:

$$w = N\delta H u \Delta p_{ch} \tag{9}$$

where, in laminar flow regime, the pressure loss throughout the heat sink is given by Kays *et al.* [17]:

$$\Delta p_{ch} = \frac{K\rho_f u^2}{2} + \frac{48\mu L u}{{D_h}^2} \tag{10}$$

where K is contraction and expansion loss coefficient for flow at heat exchanger entrance and exit, respectively. In this study the fin thickness is small compared to the channel width, where, the average ratio of the optimal channel width to the optimal fin thickness is $2.23 < \delta/\mathrm{b} < 9.39$ at the considered substrate areas and in the studied range of pumping power. Therefore the first term in Eq.10 can be neglected. By this simplification the pressure loss relation to the velocity becomes linear. The mass of heat sink depends to the channel width, channel height and fin thickness. Based on these dimensions of the heat sink, the mass of the heat sink is:

$$M_{hs} = \rho_{hs} HWL\left(1 - \frac{\delta}{b + \delta}\right) \tag{11}$$

Note that, to calculate the mass of the heat sink, the substrates of the heat sink are neglected. In this study the cost performance of the heat sink is defined as follows:

$$P = \left(R_{th}.M_{hs}\right)^{-1} \tag{12}$$

PARAMETRIC CONCERNS

The optimum dimensions of the channel and the fin are calculated for three heat sink substrate sizes ($A_s = 1\ \mathrm{cm} \times 1\ \mathrm{cm},\ 2\ \mathrm{cm} \times 2\ \mathrm{cm},$ and $3\ \mathrm{cm} \times 3\ \mathrm{cm}$). The range of the channel dimensions is in micro scale, so that the minimum and maximum values for the dimension are taken 1 μm and 1 mm, respectively. The range of the pumping power for optimizing the considered parameters is from 0.001 W to 20 W.

For a fixed pumping power, different channel dimensions and fin thickness give different Reynolds numbers. For the optimum dimensions achieved in this work, the flow regime is laminar in the studied pumping power range. Li *et al.* [18] reported that transition to the turbulence regime flow began near $\mathrm{Re} = 1535$ in micro-scale channels, which is lower than predicted Reynolds number by classical theory. Therefore, the range of the Reynolds number guarantees that the produced flows in the microchannel are in laminar regime flow throughout this study.

In this study, because of variation of the optimum dimensions of the heat sink, the thermal entry length, which sketches the boundary between the fully developed heat flow and the non-fully developed heat flow in the microchannel, varies slowly compared to variation of the pumping power. At the studied range of pumping power (from 10^{-3} W to 20 W), and by considering the channel dimensions, number of the channels, the Prandtl number, and average fluid temperature, the thermal entry length varies from 7.5×10^{-4} m to 1.7×10^{-3} m in this study. Therefore, the flow in this study can be considered fully developed thermally, where the thermal entry length is less than 17% of the total channel length. As Morini [19] stated, the entrance effects on the average Nusselt number can be neglected if the Graetz number is less than 10 ($Gz < 10$) in the microchannels. Since the variation of the Graetz number in this work is $1.58 < Gz < 7.86$, the Nusselt number is considered independent of the channel entrance effect. Water is used as coolant fluid in the aluminum heat sink. The thermal properties of the water are taken constant at 305 K. Table 1 presents the thermal properties of the coolant fluid and heat sink.

Table 1 Thermal properties of the coolant fluid and heat sink.

Parameter	C_p	k_f	ρ_f	Pr
Dimension	(J/kg. K)	(W/m . K)	(kg/m^3)	
Value	4178	0.62	999	5.2
Parameter	μ	ρ_hs	k_hs	
Dimension	$(N.s/m^2)$	(kg/m^3)	(W/m . K)	
Value	769×10^{-6}	2702	220	

RESULTS

The thermal resistance of a single channel is compared with results of finite volume method and the computational fluid dynamic (CFD) solver, FLUENT. Figure 2 shows variation of the thermal resistance with the pumping power in a single channel. The dimensions of the fin thickness, channel width, and its height are 40 μm, 400 μm, and 800 μm, respectively. Percent error between two calculations is 1.51% and 12.19% in the studied range of the thermal resistance.

In recent years the technological applications in thermo-fluids require high rates of heat transfer in relatively small spaces and volumes. In this work, to design a compact and light heat sink and to consider the heat dissipation capability of the heat sink, the cost performance and the thermal resistance of the heat sink are discussed, respectively. For case of graphical visualization, the thermal conductance of the heat sink (U), which is the reciprocal heat sink thermal resistance ($U = 1/R_{th}$) is presented.

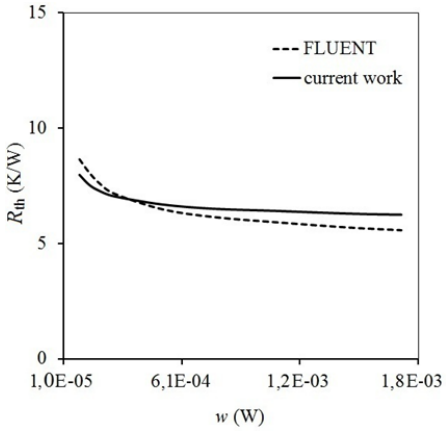

Figure 2 Thermal resistance of the microchannel heat sink compared with results of the computational fluid dynamic solver (FLUENT).

Thermal resistance

Figure 3 and Figure 4 show the variation of the thermal conductance in logarithmic scale with the channel width, fin thickness and channel height at fixed pumping power. For the 1 cm × 1 cm heat sink, the higher thermal resistance happens at smaller values of the channel width and fin thickness. As the channel height increases, the optimum thermal resistance happens at lower channel width. As can be seen in Figure 4, at fixed channel height and fixed fin thickness the lower thermal resistance happens at the lower channel width as pumping power increases. This kind of dependency is shown by Hendricks [20], where dependency of the heat sinks overall heat transfer on the microchannel design specifics is studied. To check the size effect of substrate plate on the optimum value of the channel dimensions, two sizes of the substrate plate, where $H = 100$ µm, and $b = 30$ µm, are evaluated. Figure 5 reveals that a larger heat sink changes the optimum channel dimensions, which lead to minimum thermal resistance. Compared to the smaller heat sink, the minimum thermal resistance switches to a larger channel width at a fixed pumping power in a larger heat sink.

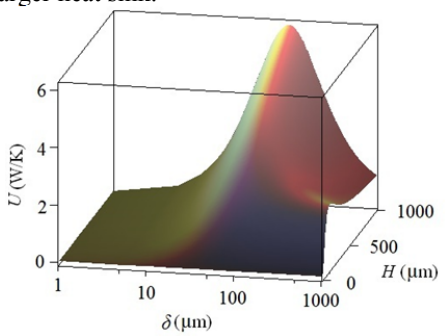

Figure 3 Variation of the thermal conductance in logarithmic scale with the channel width and channel height. b = 20 µm, w = 0.01 W, A_s = 1 cm × 1 cm.

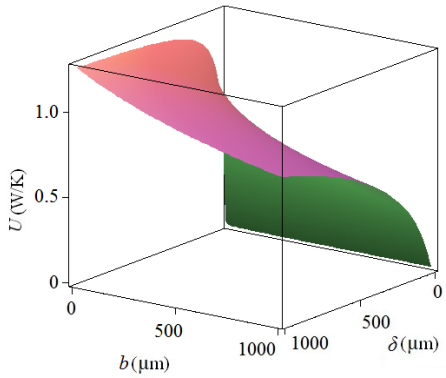

Figure 4 Variation of the thermal conductance in logarithmic scale with the channel width and fin thickness. b = 20 µm, w = 0.01 W, A_s = 1 cm × 1 cm.

Figure 6 illustrates optimum values of the wall thicknesses at studied range of the channel height that provide minimum thermal resistance. When the channel height becomes larger, the optimum thermal resistance occurs at a larger fin thickness. As a function of the channel width, there is not a global minimum value for the thermal resistance in a certain range of the fin thickness and the pumping power. For instance, at $H = 30$ µm, and 1 µm $\leq \delta \leq 1$ mm, the thermal resistance decreases as the fin thickness becomes larger, however, it is observed that the cases where w ≥ 4 .5 W, the thermal resistance has global minimum value.

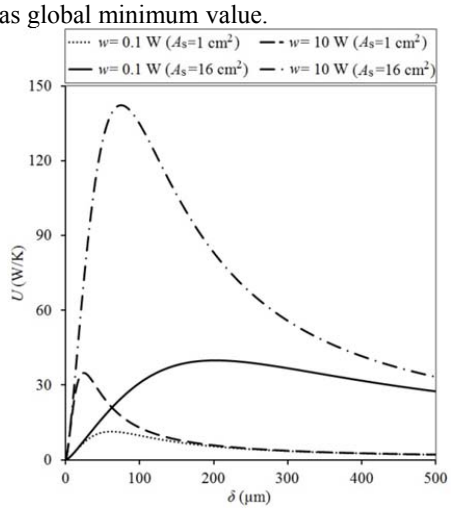

Figure 5 Variation of the thermal conductance with the channel width at two pumping powers and two substrate plate areas. H = 100 µm, b = 30 µm.

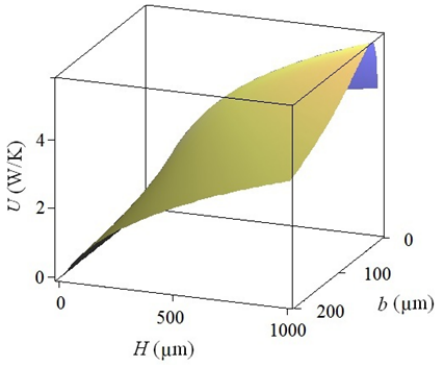

Figure 6 Variation of the thermal conductance with the channel height and fin thickness. δ = 70 μm, w = 0.01 W.

By using an effective numeric test, the heat sink can be optimized for various dimensional parameters in order to produce a minimum thermal resistance. Figure 7 shows the minimum thermal resistance at different pumping power and the variation of the cost performance in order to have the minimum thermal resistance. As is expected, the thermal resistance decreases when the pumping power increases. At any channel width and fin thickness, the larger channel height produces smaller thermal resistance due to increase in channel surface area. The channel height is taken 1 mm in the numerical test, where the maximum channel height in the studied domain. There are specific values of the channel width and fin thickness at any pumping power that produce minimum thermal resistance in the heat sink (Figure 8). The larger substrate plate of the heat sink results lower thermal resistance, due to effect of channel length and number of the channels in the heat sink. In addition, in studied range of the pumping power, the optimum channel width and fin thickness increases with the size of the substrate plate.

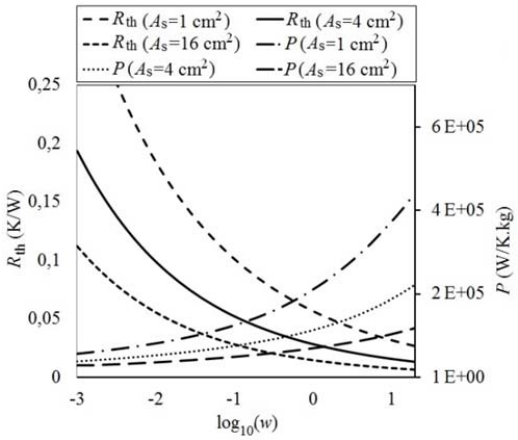

Figure 7 Cost performance and the minimum values of the heat sink thermal resistance with variation of the pumping power at three sizes of the substrate plate. A_s = 1 cm × 1 cm, 2 cm × 2 cm, and 3 cm × 3 cm.

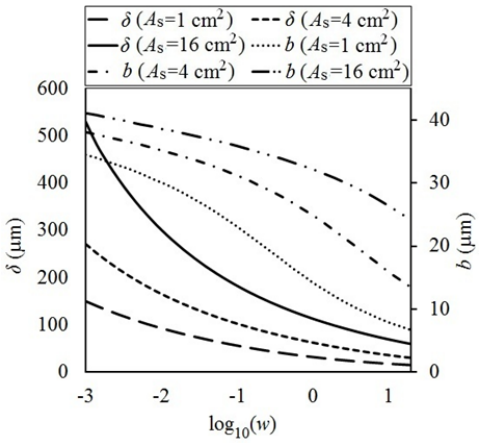

Figure 8 Optimum channel width and fin thickness with variation of the pumping power at three sizes of the substrate plate in order to produce the minimum thermal resistance. A_s = 1 cm × 1 cm, 2 cm × 2 cm, and 3 cm × 3 cm.

Cost performance

It can be noted from Figure 9 that, as the channel height varies at a fixed channel width and pumping power, there is a maximum value of the cost performance. Furthermore, at a fixed pumping power, variation of the channel width does not affect the channel height value, where the maximum cost performance occurs. Although the larger channel width provides better cost performance of the heat sink, the fin thickness should be as small as possible. Therefore, the optimum cost performance happens at a constant fin thickness when the channel height varies at a fixed pumping power. In addition, when the fin thickness becomes smaller, the optimum cost performance happens at a smaller channel height. Figure 10 shows that, the maximum cost performance occurs at a smaller channel height when the pumping power increases.

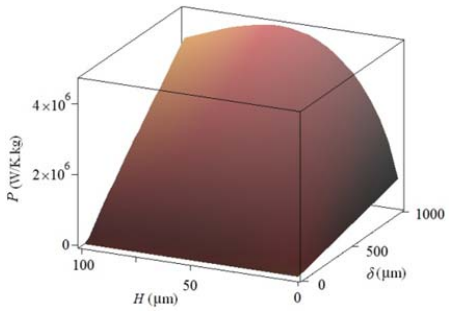

Figure 9 Variations of the cost performance with the channel width and channel height. b = 20 μm, w = 0.01 W.

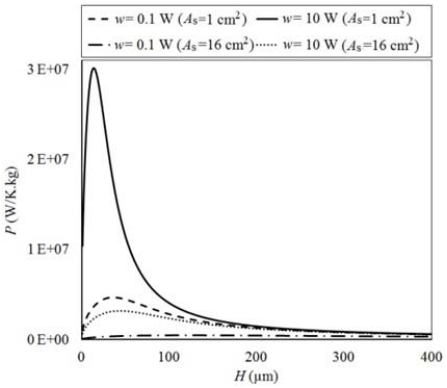

Figure 10 Variation of the cost performance with the channel height at four pumping powers. $\delta = 70$ μm, $b = 100$ μm.

According to the Eq. 11, at fixed heat sink substrate dimensions, the mass of the heat sink is defined based on the channel dimensions and the fin thickness. The maximum cost performance can be obtained by Eq. 12. This equation includes both the thermal resistance and mass of the heat sink. This equation reveals that, when the fin thickness goes to zero the cost performance tends to infinity. On the other hand, decreasing the fin thickness means that the channel width increases at fixed heat substrate width. Since the channel dimensions (δ, H and b) are limited in micro scale range, the channel width and the fin thickness are fixed at 1μm and 1mm, respectively. As is mentioned, larger channel height produces lower thermal resistance, but it increases the mass of the heat sink (Eq. 11). Therefore, there should be an optimum value of the channel height that provides the maximum cost performance at any pumping power. Figure 11 illustrate that, when the pumping power increases, the optimum channel height becomes smaller that generates a maximum cost performance. The size of the channel height affects the fin efficiency and the mass of the heat sink, where both of these parameters define the cost performance. Therefore, the cost performance is dependent on the channel height. Because a larger substrate plate leads to higher channel height in maximization of the cost performance of the heat sink (Figure 12), the cost performance decreases, due to an increase in heat sink mass.

As the maximum cost performance does not occur at the minimum thermal resistance and the dimensions of the channel and fin thickness are different at a fixed pumping power, the produced Reynolds numbers at maximum cost performance and minimum thermal resistance are also different. For optimizing of the thermal resistance, the number of the microchannels increases with the pumping power, due to the smaller channel width and smaller fin thickness, while the number of the microchannels is taken fixed in the cost performance optimization. Therefore, as can be seen in Figure 13, the Reynolds number increases slower with the pumping power at the minimum thermal resistance, compared with the Reynolds number at the maximum cost performance. In the studied range of the pumping power, the number of the microchannels varies from 45 to 453 for optimizing of the thermal resistance of the eat sink.

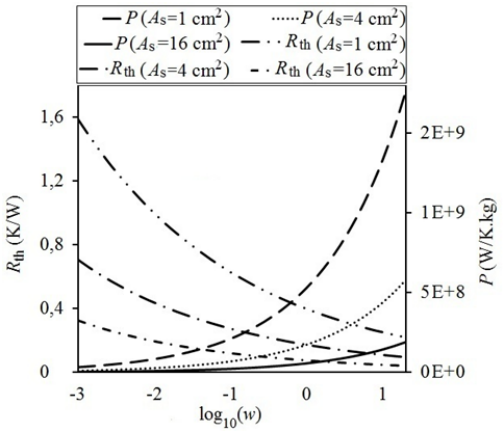

Figure 11 Thermal resistance and the optimum cost performance of the heat sink with variation of the pumping power at three sizes of the substrate plate. $A_s = 1$ cm × 1 cm, 2 cm × 2 cm, and 3 cm × 3 cm.

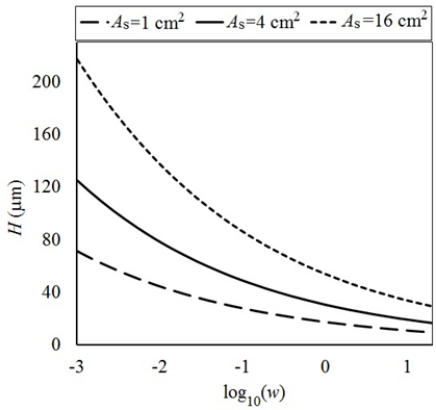

Figure 12 Optimum channel height variations with the pumping power at three sizes of the substrate plate in order to produce the maximum cost performance. $A_s = 1$ cm × 1 cm, 2 cm × 2 cm, and 3 cm × 3 cm.

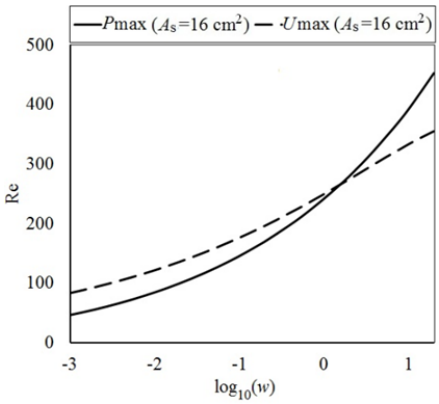

Figure 13 The Reynolds number variations with the pumping power at the minimum thermal resistance and the maximum cost performance.

CONCLUSIONS

In order to minimize the thermal resistance and to maximize the cost performance of a micro plate-fin heat sink, the channel width, the channel height and the fin thickness are optimized at a wide range of pumping power. The analytical approach in this work generated some equations based on the flow and heat transfer characteristics in the laminar flow regime. The results discuss the effect of three sizes of the substrate plate on optimized size of the channel and fin thickness. To minimize the thermal resistance results show that the larger substrate plate switches the minimum thermal resistance to the larger channel width and the larger channel height produces a smaller thermal resistance. In addition, at any studied pumping power, there are specific values of the channel width and fin thickness which produce minimum thermal resistance in the heat sink. The results which are generated for the detailed description of the cost performance, illustrate that a larger channel width and a smaller fin thickness lead to a better cost performance. In addition, the optimum channel height decreases as the pumping power increases.

ACKNOWLEDGMENTS

The authors would like to acknowledge the Center for Energy Materials (CEM) that this work is carried in this center in collaboration with Aarhus University, Denmark. This work is funded in part by the Danish Council for Strategic Research, Programme Commission on Energy and Environment, under Grant No 823032.

REFERENCES

[1] Schubert K., Brandner J., Fichtner M., Linder G., Schygulla U., and Wenka A., Microstructure devices for applications in thermal and chemical process engineering, *Nanoscale and Microscale Thermophysical Engineering,* vol. 5, no.1 pp. 17-39, 2010.

[2] Rezania A., and Rosendahl L. A., Thermal effect of a thermoelectric generator on parallel microchannel heat sink, *Energy*, vol. 37, no.1, pp. 220-227, 2012.

[3] Rosa P., Karayiannis T. G., and Collins M. W., Single-phase heat transfer in microchannels: The importance of scaling effects, *Applied Thermal Engineering,* vol. 29 no. 17-18, pp. 3447-3468, 2009.

[4] Peng X. F., and Peterson G. P., Convective heat transfer and flow friction for water flow in microchannel structures, *International Journal of Heat and Mass Transfer*, vol. 39, no. 12, pp. 2599-2608, 1996.

[5] Gunnasegaran P., Mohammed H. A., Shuaib N. H., and Saidur R., The effect of geometrical parameters on heat transfer characteristics of microchannels heat sink with different shapes, *International Journal of Heat and Mass Transfer*, vol. 37, no. 8, pp. 1078-1086, 2010.

[6] Chen Y., Zhang C., Shi M., and Wu J., Three-dimensional numerical simulation of heat and fluid flow in noncircular microchannel heat sinks, *International Communications in Heat and Mass Transfer,* vol. 36, no. 9, pp. 917-920, 2009.

[7] Kroeker C. J., Soliman H. M., and Ormiston S. J., Three-dimensional thermal analysis of heat sinks with circular cooling micro-channels, *International Journal of Heat and Mass Transfer,* vol. 47, no. 22, pp. 4733-4744, 2004.

[8] Kou H., Lee J., and Chen C., Optimum thermal performance of microchannel heat sink by adjusting channel width and height, *International Communications in Heat and Mass Transfer*, vol. 35, no. 5, pp. 577-582, 2008.

[9] Tuckerman D. B., and Pease R. F. W., High-performance heat sinking for VLSI, *IEEE Electron Device Letters,* vol. 2, no. 5, pp. 126-129, 1981.

[10] Hendricks T. J., Micro- and nano-technologies: roadmap enabling more compact, lightweight thermoelectric power generation and cooling systems, *Proc. ASME 2011, 9th International Conference Nanochannels, Microchannels, and Minichannels,* Paper # ICNMM2011-58286, Edmonton, Alberta, Canada, 2011.

[11] Hendricks T. J., Microtechnology – a key to system miniaturization in advanced energy recovery & conversion systems, *Proc. ASME 2008, 2nd International Conference on Energy Sustainability,* Paper #ES2008-54244, Jacksonville, FL, 2008.

[12] Yazawa K., and Shakouri A, Cost-efficiency trade-off and the design of thermoelectric power generators, *Environmental Science & Technology,* vol. 45, no. 17, pp. 7548-7553, 2011.

[13] Kim D., and Kim S. J., Averaging approach for microchannel heat sinks subject to the uniform wall temperature condition, *International Journal of Heat and Mass Transfer,* vol. 49, no. 3-4, pp. 695-706, 2006.

[14] Kim S. J., Methods for Thermal Optimization of Microchannel Heat Sinks, *Heat Transfer Engineering,* vol. 25, no.1, pp. 37-49, 2004.

[15] Dharaiya V.V., and Kandlikar S.G., Numerical investigation of heat transfer in rectangular microchannels under H2 boundary condition during developing and fully developed laminar flow, *Journal of Heat Transfer,* vol. 134, pp. 020911-1, 2012.

[16] Incropera F. P., and DeWitt D. P., *Fundamentals of heat and mass transfer,* 6th ed. pp. 137-154, John Wiley and Sons, New York, 1996.

[17] Kays W. M., Crawford M. E., and Weigand B., *Convective heat and mass transfer,* 4th ed., McGraw-Hill Higher Education, Princeton 2004.

[18] Li H., Ewoldt R., and Olsen M. G., Turbulent and transitional velocity measurements in a rectangular microchannel using microscopic particle image velocimetry, *Experimental Thermal and Fluid Science,* vol. 29, no. 4, pp. 435-446, 2005.

[19] Morini G. L., Scaling effects for liquid flows in microchannels, *Heat Transfer Engineering,* vol. 27, no. 4, pp. 64-73, 2006.

[20] Hendricks T. J., Microchannel & minichannel heat exchangers in advanced energy recovery & conversion systems, *Proc. ASME 2006, International Mechanical Engineering Congress & Exposition,* Paper #IMECE2006-14594, Chicago, IL, 2006.